Computational Methods for Ideal Magnetohydrodynamics

Andrew Kercher

A defense of the dissertation submitted in partial fulfillment of the requirements
for the degree of Doctor of Philosophy
George Mason University

25 August 2014

Introduction

- Solutions to Riemann problems of hydrodynamics and ideal magnetohydrodynamics.

Introduction

- Solutions to Riemann problems of hydrodynamics and ideal magnetohydrodynamics.
- High resolution schemes produce incorrect results for coplanar and near coplanar Riemann problems of ideal MHD.

Introduction

- Solutions to Riemann problems of hydrodynamics and ideal magnetohydrodynamics.
- High resolution schemes produce incorrect results for coplanar and near coplanar Riemann problems of ideal MHD.
- Explanation of why these problems are difficult for conservative numerical schemes based on a finite volume discretization.

Introduction

- Solutions to Riemann problems of hydrodynamics and ideal magnetohydrodynamics.
- High resolution schemes produce incorrect results for coplanar and near coplanar Riemann problems of ideal MHD.
- Explanation of why these problems are difficult for conservative numerical schemes based on a finite volume discretization.
- Description of new method called compound wave modification (CWM) that corrects the inaccuracies.
  - Modifies the HLLD flux.
  - Converges at all grid resolutions.
  - Reduces error by 6 to 25 times.

Introduction

- Solutions to Riemann problems of hydrodynamics and ideal magnetohydrodynamics.
- High resolution schemes produce incorrect results for coplanar and near coplanar Riemann problems of ideal MHD.
- Explanation of why these problems are difficult for conservative numerical schemes based on a finite volume discretization.
- Description of new method called compound wave modification (CWM) that corrects the inaccuracies.
    - Modifies the HLLD flux.
    - Converges at all grid resolutions.
    - Reduces error by 6 to 25 times.
- Description multi-dimensional fluid solvers capable of shared memory parallelism.

Riemann Problems

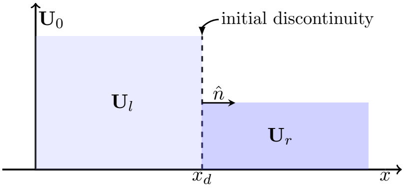

- Initial discontinuity at x_d separates two constant states.

$$\frac{\partial \mathbf{U}}{\partial t} + \frac{\partial \mathbf{F}}{\partial \mathbf{x}} = \mathbf{0} \ ,$$

$$\mathbf{U}_0 = \begin{cases} \mathbf{U}_l & \text{if} \quad x < x_d, \\ \mathbf{U}_r & \text{if} \quad x > x_d, \end{cases}$$

Riemann Problems

$$\frac{\partial \mathbf{U}}{\partial t} + \frac{\partial \mathbf{F}}{\partial \mathbf{x}} = \mathbf{0} \ ,$$

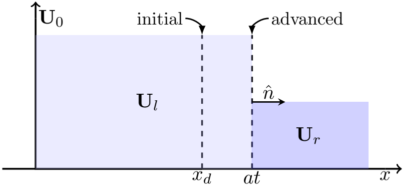

$$\mathbf{U}_0 = \begin{cases} \mathbf{U}_l & \text{if} \quad x < x_d, \\ \mathbf{U}_r & \text{if} \quad x > x_d, \end{cases}$$

- Solution at time t.
- Wave speed: a.

$$\mathbf{U} = \begin{cases} \mathbf{U}_l & \text{if} \quad x < at, \\ \mathbf{U}_r & \text{if} \quad x > at, \end{cases}$$

Riemann Problems

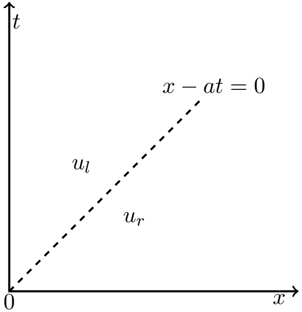

$$\frac{\partial u}{\partial t} + a\frac{\partial u}{\partial x} = \mathbf{0} \ ,$$

$$u_0 = \begin{cases} u_l & \text{if} \quad x < x_d, \\ u_r & \text{if} \quad x > x_d, \end{cases}$$

- Linear advection, $\mathbf{U}_l = u_l$ and $\mathbf{U}_r = u_r$.
- Self-similar solution in (x, t)-plane.

$$u = \begin{cases} u_l & \text{if} \quad x < at, \\ u_r & \text{if} \quad x > at, \end{cases}$$

Riemann Problems: Systems of linear equations

- Hyperbolic $\rightarrow$ real eigenvalues, $\lambda_1, \ldots, \lambda_n$, and linearly independent right eigenvectors, $\mathbf{r}^1, \ldots, \mathbf{r}^n$.
- Strictly hyperbolic $\rightarrow$ distinct eigenvalues.

$$\frac{\partial \mathbf{U}}{\partial t} + \mathbf{A}\frac{\partial \mathbf{U}}{\partial x} = 0,$$

Riemann Problems: Systems of linear equations

- Hyperbolic $\rightarrow$ real eigenvalues, $\lambda_1, \ldots, \lambda_n$, and linearly independent right eigenvectors, $\mathbf{r}^1, \ldots, \mathbf{r}^n$.
- Strictly hyperbolic $\rightarrow$ distinct eigenvalues.
- Characteristic form, $\mathbf{W} = \mathbf{l}^i \mathbf{U}$, where $\mathbf{l}^i$ is the matrix of left eigenvectors.

$$\frac{\partial \mathbf{U}}{\partial t} + \mathbf{A} \frac{\partial \mathbf{U}}{\partial x} = 0,$$

$$\frac{\partial \mathbf{W}}{\partial t} + \mathbf{\Lambda} \frac{\partial \mathbf{W}}{\partial x} = 0,$$

Riemann Problems: Systems of linear equations

- Hyperbolic $\rightarrow$ real eigenvalues, $\lambda_1, \ldots, \lambda_n$, and linearly independent right eigenvectors, $\mathbf{r}^1, \ldots, \mathbf{r}^n$.
- Strictly hyperbolic $\rightarrow$ distinct eigenvalues.
- Characteristic form, $\mathbf{W} = \mathbf{l}^i\mathbf{U}$, where $\mathbf{l}^i$ is the matrix of left eigenvectors.
- n scalar equations.

$$\frac{\partial \mathbf{U}}{\partial t} + \mathbf{A}\frac{\partial \mathbf{U}}{\partial x} = 0,$$

$$\frac{\partial \mathbf{W}}{\partial t} + \mathbf{\Lambda}\frac{\partial \mathbf{W}}{\partial x} = 0,$$

$$\frac{\partial w_i}{\partial t} + \lambda_i\frac{\partial w_i}{\partial x} = 0,$$

Riemann Problems: Systems of linear equations

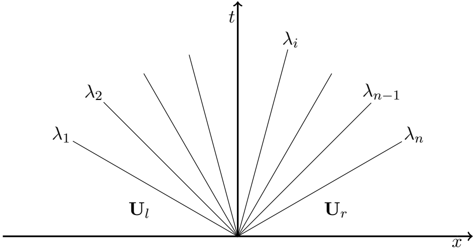

- Self-similar solutions for a system of linear waves.

- Difference across each wave $\alpha_i = \mathbf{l}_i \cdot (\mathbf{U}_l - \mathbf{U}_r)$.

Riemann Problems: Systems of linear equations

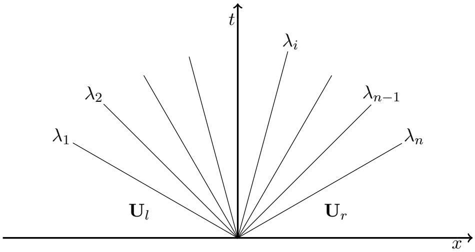

- Self-similar solutions for a system of linear waves.
- Information is global, state across each wave is known.

- Difference across each wave $\alpha_i = \mathbf{l}_i \cdot (\mathbf{U}_l - \mathbf{U}_r)$.
- In terms of conservative variables

$$\mathbf{U} = \mathbf{U}_l + \sum_{i=1}^{m} \alpha_i \mathbf{r}^i$$

or

$$\mathbf{U} = \mathbf{U}_r - \sum_{i=m+1}^{n} \alpha_i \mathbf{r}^i$$

Riemann Problems: Systems of nonlinear equations

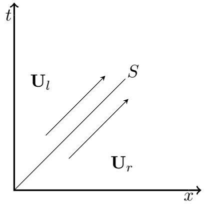

$$\frac{\partial \mathbf{U}}{\partial t} + \frac{\partial \mathbf{F}}{\partial x} = 0,$$

- linear wave, characteristics parallel.

Riemann Problems: Systems of nonlinear equations

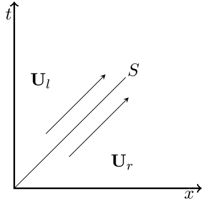

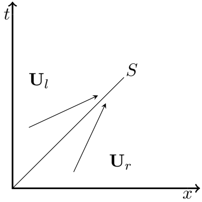

$$\frac{\partial \mathbf{U}}{\partial t} + \frac{\partial \mathbf{F}}{\partial x} = 0,$$

- linear wave, characteristics parallel.
- Shock wave, compression, characteristics converge.

Riemann Problems: Systems of nonlinear equations

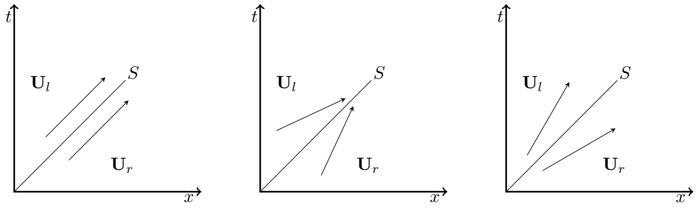

$$\frac{\partial \mathbf{U}}{\partial t} + \frac{\partial \mathbf{F}}{\partial x} = 0,$$

- linear wave, characteristics parallel.
- Shock wave, compression, characteristics converge.
- Rarefaction wave, expansion, characteristics diverge.

Riemann Problems: Systems of nonlinear equations

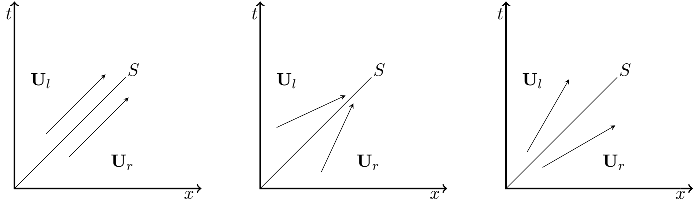

$$\frac{\partial \mathbf{U}}{\partial t} + \frac{\partial \mathbf{F}}{\partial x} = 0,$$

- linear wave, characteristics parallel.
- Shock wave, compression, characteristics converge.
- Rarefaction wave, expansion, characteristics diverge.
- Information only local, state each across wave unknown.

Compressible hydrodynamics

$$
\begin{aligned}
\frac{\partial \rho}{\partial t} + \nabla \cdot (\rho \mathbf{v}) = 0 \ , \\
\frac{\partial (\rho \mathbf{v})}{\partial t} + \nabla \cdot [\rho \mathbf{v} \otimes \mathbf{v} + p_g] = 0 \ , \\
\frac{\partial E}{\partial t} + \nabla \cdot [(E + p_g)\, \mathbf{v}] = 0 \ ,
\end{aligned}
$$

where the energy density is defined as

$$
E = \frac{p_g}{\gamma - 1} + \frac{\rho v^2}{2} \ ,
$$

Compressible hydrodynamics

The Euler equations are strictly hyperbolic.
1D conservative form

$$\frac{\partial \mathbf{U}}{\partial t} + \frac{\partial \mathbf{F}}{\partial x} = 0.$$

Jacobian $\mathbf{J}(\mathbf{U}) = \partial \mathbf{F}/\partial \mathbf{U}$ has three real and distinct eigenvalues:

$$\begin{aligned} \lambda_3 &= v_n + a : \text{rarefaction or shock} \\ \lambda_2 &= v_n \qquad : \text{contact discontinuity} \\ \lambda_1 &= v_n - a : \text{rarefaction or shock} \end{aligned}$$

where $a = \sqrt{\gamma p_g/\rho}$ is the speed of sound.

Compressible hydrodynamics

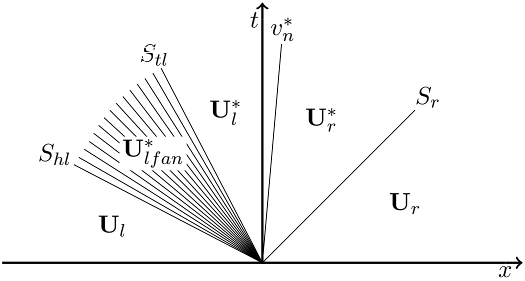

$\lambda_3 = S_l$: rarefaction

$\lambda_2 = v_n^*$: contact discontinuity

$\lambda_1 = S_r$: shock

Compressible hydrodynamics

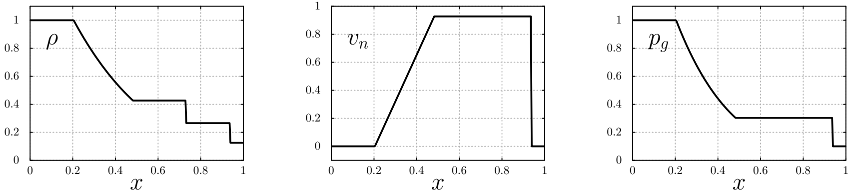

- Exact solution to Sod shock tube problem [7].

Compressible hydrodynamics

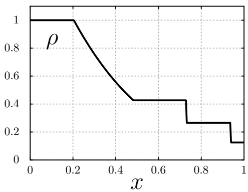

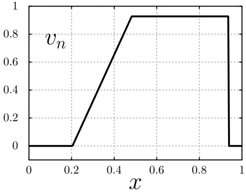

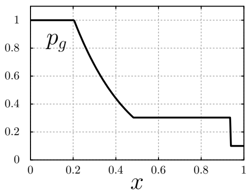

- Exact solution to Sod shock tube problem [7].
- Rarefaction head: $x \approx 0.2$.

Compressible hydrodynamics

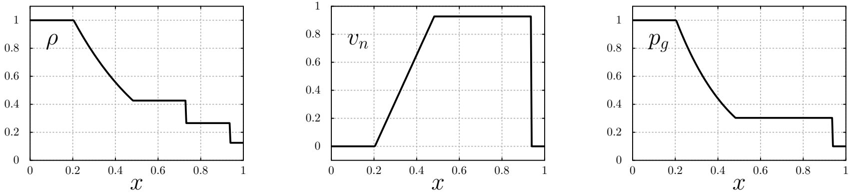

- Exact solution to Sod shock tube problem [7].
- Rarefaction head: $x \approx 0.2$.
- Rarefaction tail: $x \approx 0.45$.

Compressible hydrodynamics

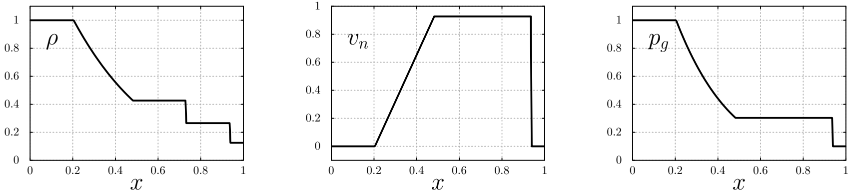

- Exact solution to Sod shock tube problem [7].
- Rarefaction head: $x \approx 0.2$.
- Rarefaction tail: $x \approx 0.45$.
- Contact discontinuity: $x \approx 0.72$.

Compressible hydrodynamics

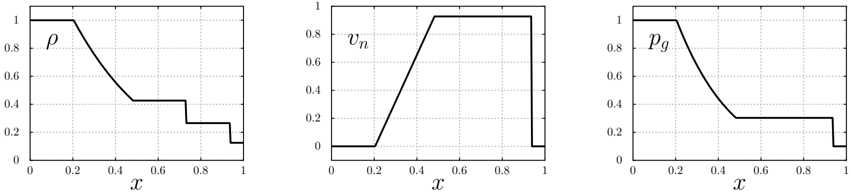

- Exact solution to Sod shock tube problem [7].
- Rarefaction head: $x \approx 0.2$.
- Rarefaction tail: $x \approx 0.45$.
- Contact discontinuity: $x \approx 0.72$.
- Shock: $x \approx 0.95$.

HLL family of approximate Riemann solvers

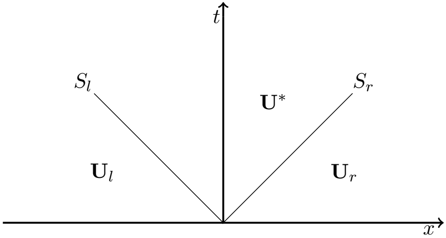

- The solver of Harden-Lax-van Leer-Einfeldt (HLLE) [1] assumes a two state solution.
- The solution approximated as weighted average of the left and right states.

HLL family of approximate Riemann solvers

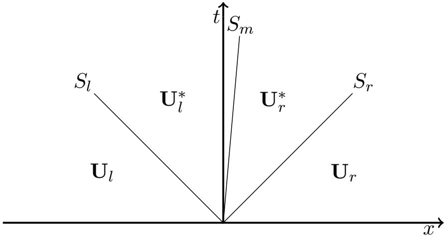

- The solver of Harden-Lax-van Leer-Einfeldt (HLLE) [1] assumes a two state solution.
- The solution approximated as weighted average of the left and right states.
- Toro, Spruce, and Speares [8] included the contact discontinuity and termed the solver HLLC.

HLL family of approximate Riemann solvers

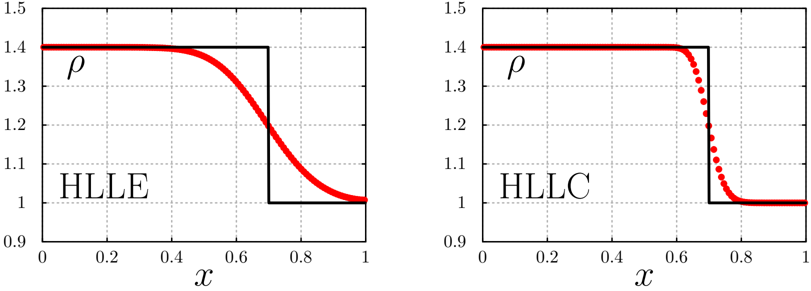

- The solver of Harden-Lax-van Leer-Einfeldt (HLLE) [1] assumes a two state solution.
- The solution approximated as weighted average of the left and right states.
- Toro, Spruce, and Speares [8] included the contact discontinuity and termed the solver HLLC.
- HLLC less diffuse at contact discontinuity.

Ideal magnetohydrodynamics

$$\frac{\partial \rho}{\partial t} + \nabla \cdot (\rho \mathbf{v}) = 0 \ ,$$

$$\frac{\partial (\rho \mathbf{v})}{\partial t} + \nabla \cdot \left[\rho \mathbf{v} \otimes \mathbf{v} + \left(p_g + \frac{B^2}{2} \right) \underline{\mathbf{I}} - \mathbf{B} \otimes \mathbf{B} \right] = 0 \ ,$$

$$\frac{\partial E}{\partial t} + \nabla \cdot \left[\left(E + p_g + \frac{B^2}{2} \right) \mathbf{v} - \mathbf{v} \cdot \mathbf{B} \otimes \mathbf{B} \right] = 0 \ , \text{ and}$$

$$\frac{\partial \mathbf{B}}{\partial t} + \nabla \cdot [\mathbf{v} \otimes \mathbf{B} - \mathbf{B} \otimes \mathbf{v}] = 0 \ ,$$

where the energy density is defined as

$$E = \frac{p_g}{\gamma - 1} + \frac{\rho v^2}{2} + \frac{B^2}{2} \ ,$$

Ideal magnetohydrodynamics

The ideal MHD equations are non-strictly hyperbolic. 1D conservative form

$$\frac{\partial \mathbf{U}}{\partial t} + \frac{\partial \mathbf{F}}{\partial x} = 0.$$

Jacobian $\mathbf{J}(\mathbf{U}) = \partial \mathbf{F} / \partial \mathbf{U}$ has seven real, but not necessarily distinct eigenvalues:

$$\begin{aligned} v_n &: \text{contact or tangential discontinuity (entropy)}, \\ v_n \pm c_s &: \text{slow rarefaction or shock}, \\ v_n \pm c_a &: \text{rotational discontinuity (Alfvén), and} \\ v_n \pm c_f &: \text{fast rarefaction or shock}, \end{aligned}$$

$$c_{f,s}^2 = \frac{1}{2}\left[a^2 + c_a^2 + c_t^2 \pm \sqrt{\left(a^2 + c_a^2 + c_t^2\right)^2 - 4a^2 c_a^2}\right],$$

$$c_a^2 = \frac{B_n^2}{\rho}, \text{ and } c_t^2 = \frac{B_t^2}{\rho}.$$

Ideal magnetohydrodynamics

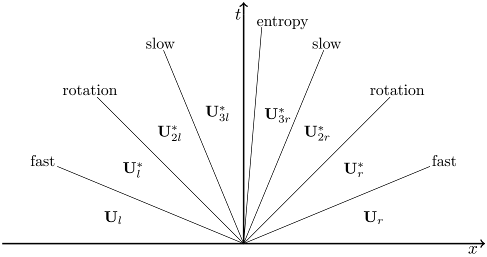

$$\begin{aligned} v_n &: \text{contact or tangential discontinuity (entropy)},\\ v_n \pm c_s &: \text{slow rarefaction or shock},\\ v_n \pm c_a &: \text{rotational discontinuity (Alfvén), and}\\ v_n \pm c_f &: \text{fast rarefaction or shock}, \end{aligned}$$

Extension of HLLC for MHD

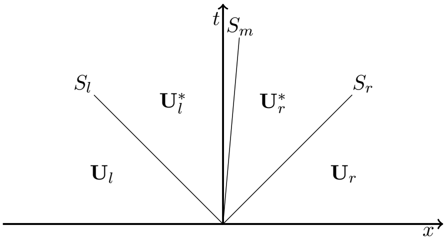

- HLLD [5] is an MHD extention to HLLC.

Extension of HLLC for MHD

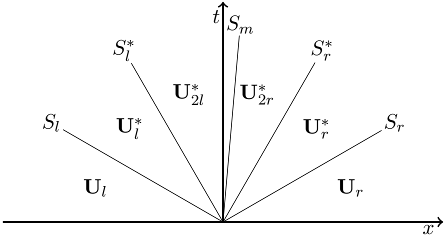

- HLLD [5] is an MHD extention to HLLC.
- Captures all linear discontinuities, contact and rotational.

Finite volume discretization

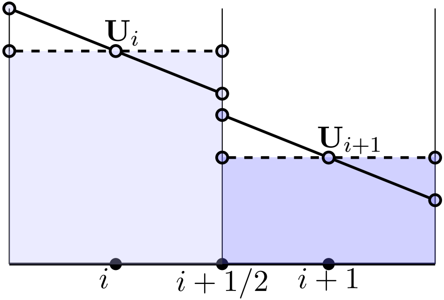

- Conservative variables are located at the cell centers.
- Flux is evaluated at cell interface.
- Flux contribution of each face added to cell.

$$\mathbf{U}^{n+1}_{\text{cell}} = \mathbf{U}^{n}_{\text{cell}} - \frac{\delta t}{V_{\text{cell}}} \sum_{\text{faces}} \mathbf{F} \cdot \mathbf{s}$$

Finite volume discretization

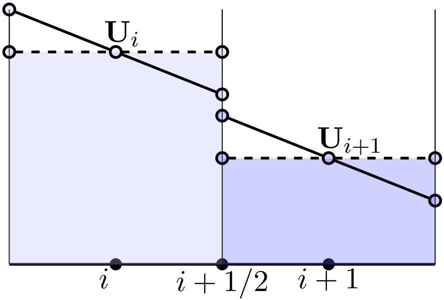

- Conservative variables are located at the cell centers.
- Flux is evaluated at cell interface.
- In 1D

$$\mathbf{U}_i^{n+1} = \mathbf{U}_i^n - \frac{\delta t}{\delta x}\left(\mathbf{F}_{i+1/2}^n - \mathbf{F}_{i-1/2}^n\right)$$

Higher order extensions

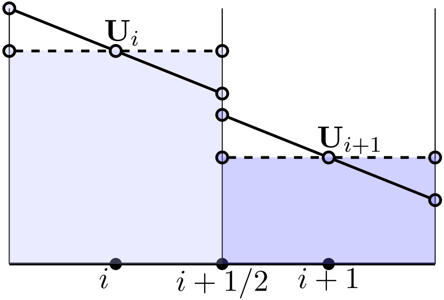

- Increase accuracy and preserve monotonicity.
- Total variation diminishing (TVD).
- Limit slope to ensure no new extrema are created.

Higher order extensions

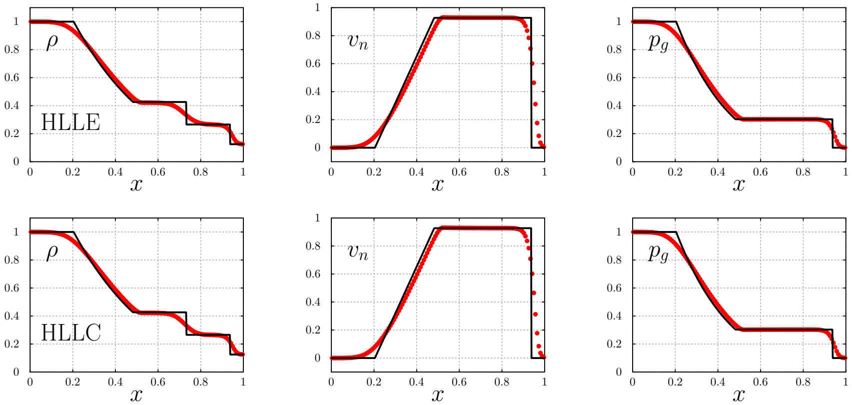

- Increase accuracy and preserve monotonicity.
- Total variation diminishing (TVD).
- Limit slope to ensure no new extrema are created.

Higher order extensions

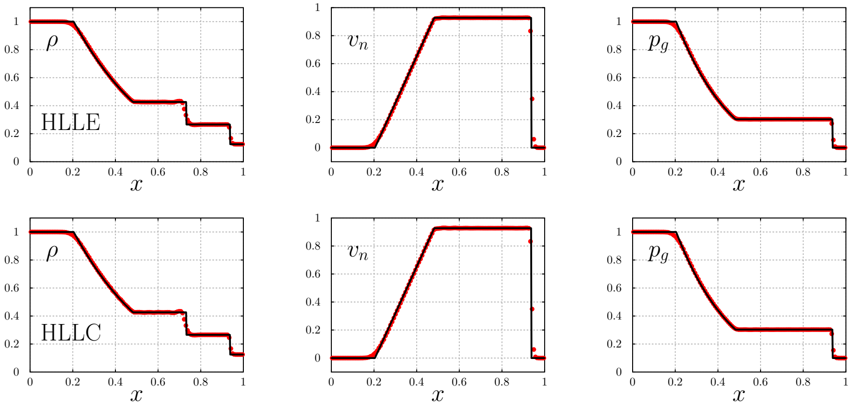

- Increase accuracy and preserve monotonicity.
- Total variation diminishing (TVD).
- Limit slope to ensure no new extrema are created.

Higher order extensions

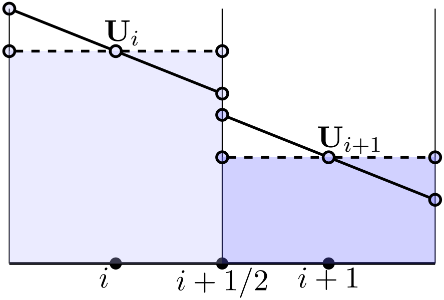

- Increase accuracy and preserve monotonicity.
- Flux corrected transport.
- Limit fluxes so that no new extrema are created.
- Higher resolution with FCT and TVD schemes.

Higher order extensions

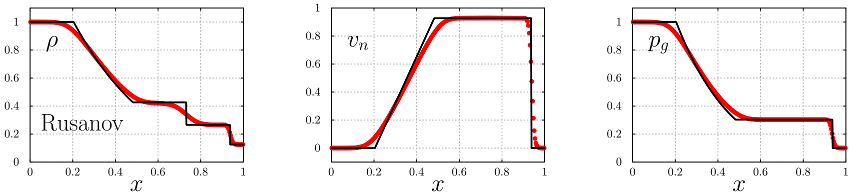

- Increase accuracy and preserve monotonicity.
- Flux corrected transport.
- Limit fluxes so that no new extrema are created.
- Higher resolution with FCT and TVD schemes.

Higher order extensions

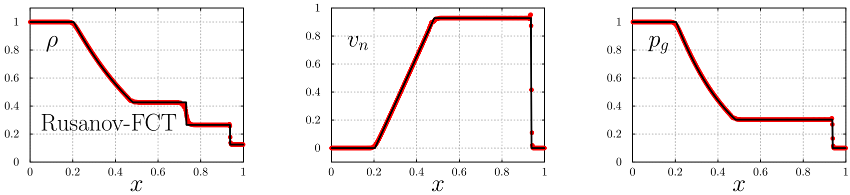

- Increase accuracy and preserve monotonicity.
- Flux corrected transport.
- Limit fluxes so that no new extrema are created.
- Higher resolution with FCT and TVD schemes.

Riemann problems for ideal MHD

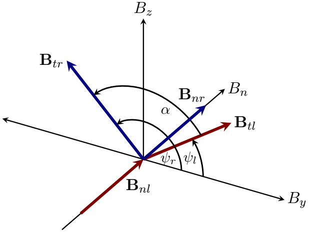

- Initial discontinuity separates two states.
- Rotation angle $\arctan B_z/B_y$.
- The initial twist angle $\alpha = \psi_r - \psi_l$.

Riemann problems for ideal MHD

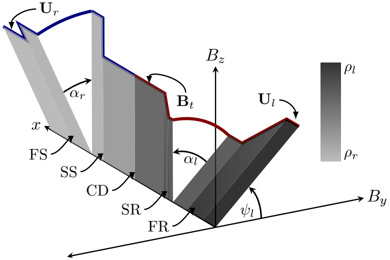

- Seven waves propagate away from initial discontinuity creating eight distinct states.

Riemann problems for ideal MHD

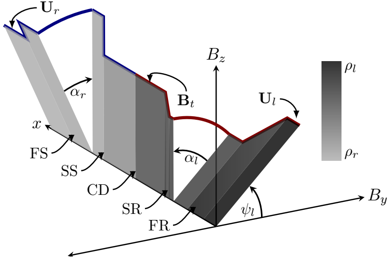

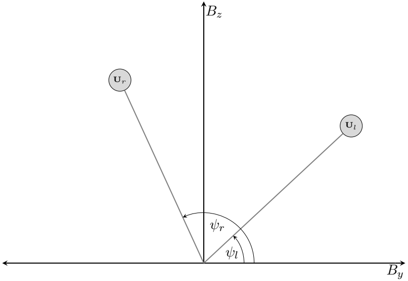

- Regular waves only alter the magnitude or orientation of B_t.

Riemann problems for ideal MHD

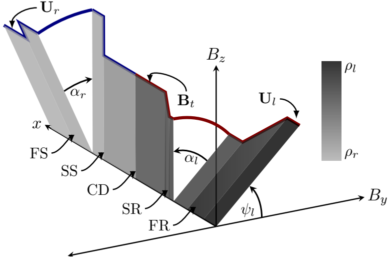

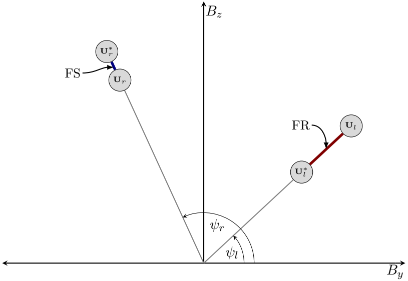

- Regular waves only alter the magnitude or orientation of B_t.
- B_t increases across fast shock, decreases across fast rarefaction.

Riemann problems for ideal MHD

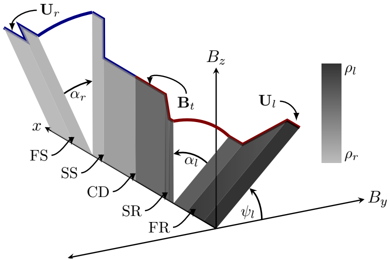

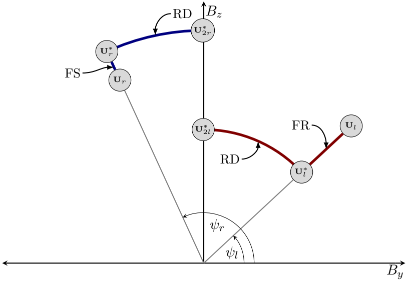

- Regular waves only alter the magnitude or orientation of B_t.
- B_t increases across fast shock, decreases across fast rarefaction.
- B_t changes orientation across a rotational discontinuity.

Riemann problems for ideal MHD

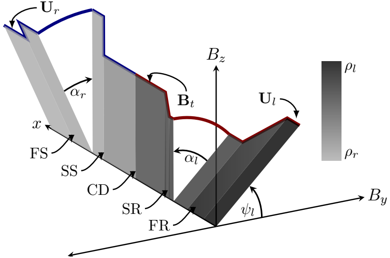

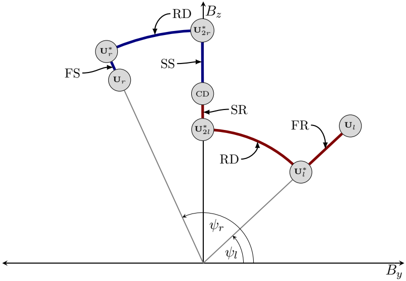

- Regular waves only alter the magnitude or orientation of B_t.
- B_t increases across fast shock, decreases across fast rarefaction.
- B_t changes orientation across a rotational discontinuity.
- B_t decreases across slow shock, increases across slow rarefaction.

Ideal MHD test problems

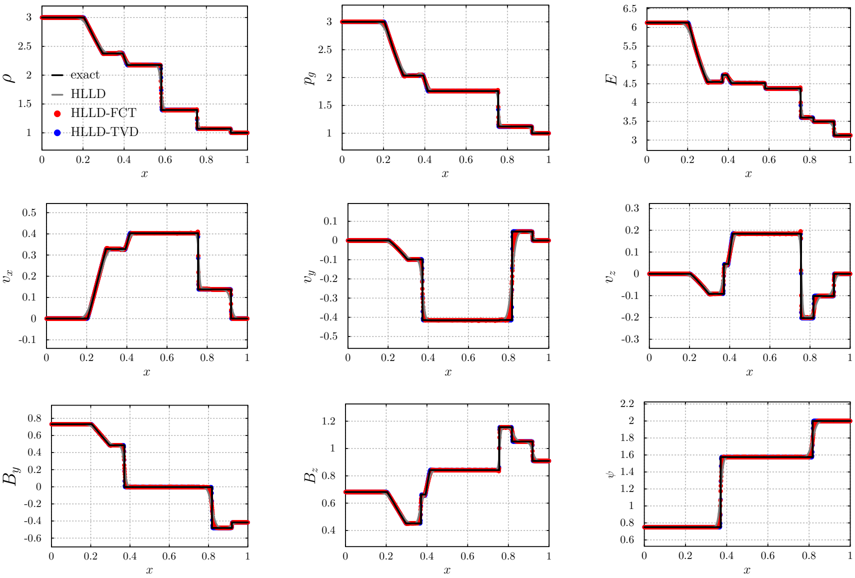

Ideal MHD test problems

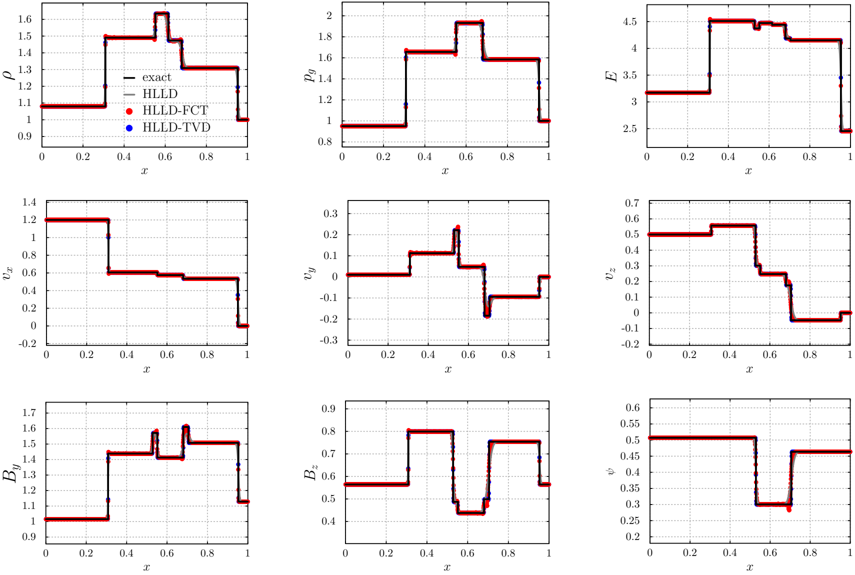

Ideal MHD test problems

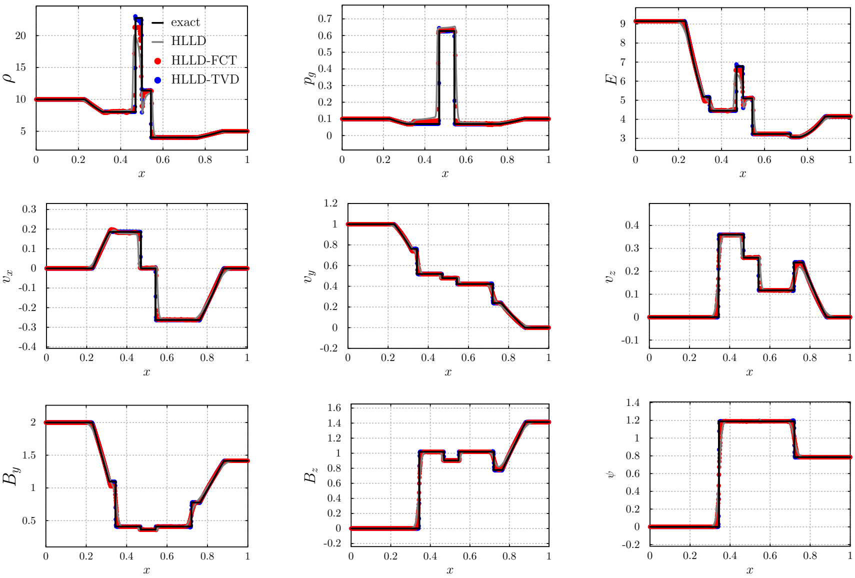

Ideal MHD test problems

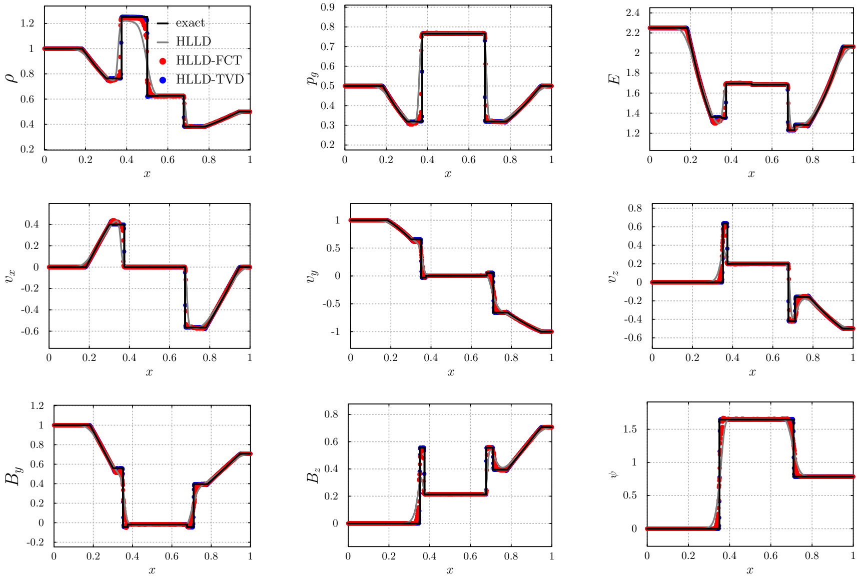

Ideal MHD test problems

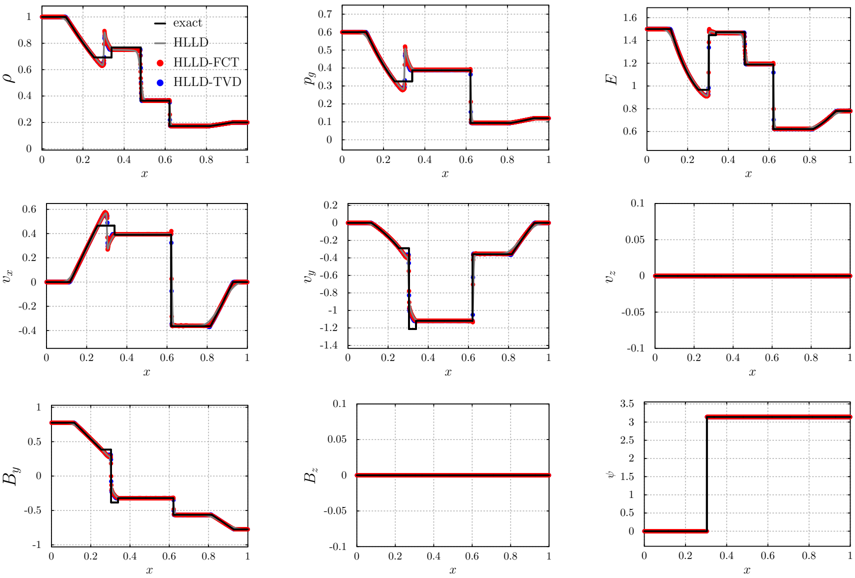

Ideal MHD test problems

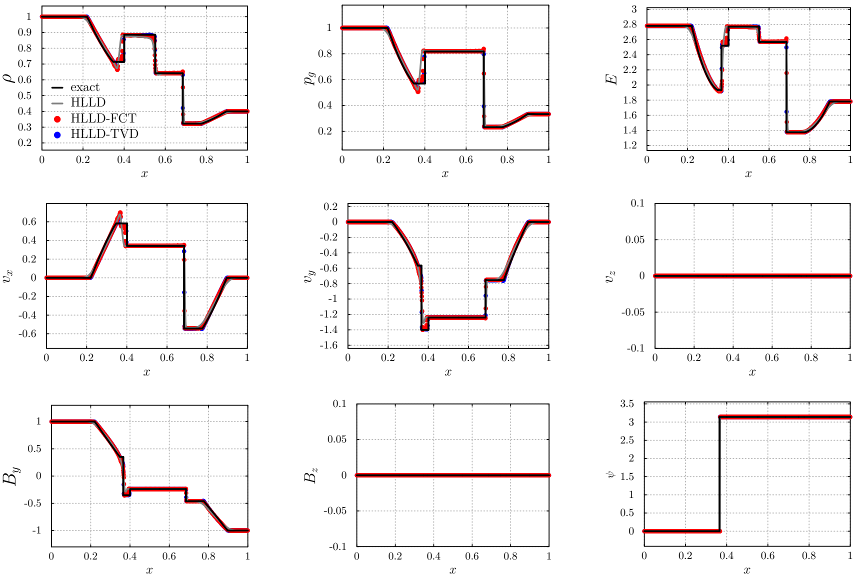

Ideal MHD test problems

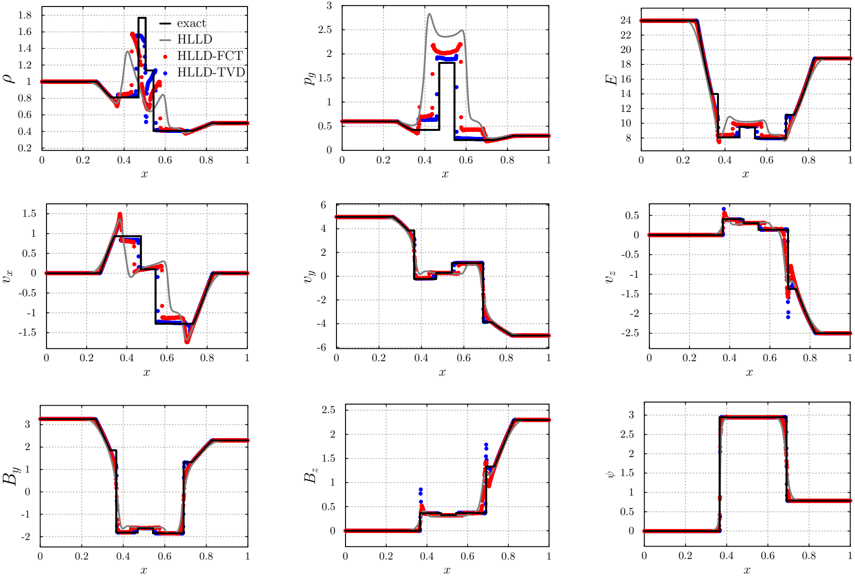

Non-unique solutions

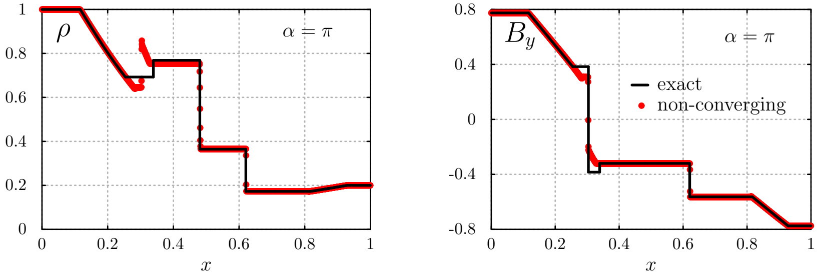

- Solutions to coplanar Riemann problems of ideal MHD are non-unique.
- At $x = 0.303$, rotational discontinuity $\rightarrow$ compound wave.

Non-unique solutions

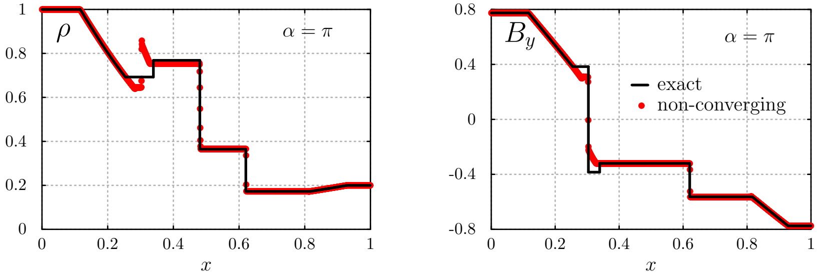

- Solutions to coplanar Riemann problems of ideal MHD are non-unique.
- At $x = 0.303$, rotational discontinuity $\rightarrow$ compound wave.
- Compound wave is composed of an intermediate shock and a slow rarefaction.
- Physical?
- Unstable for under small perturbations [4].
- Satisfies jump conditions in the coplanar case.

Non-unique solutions

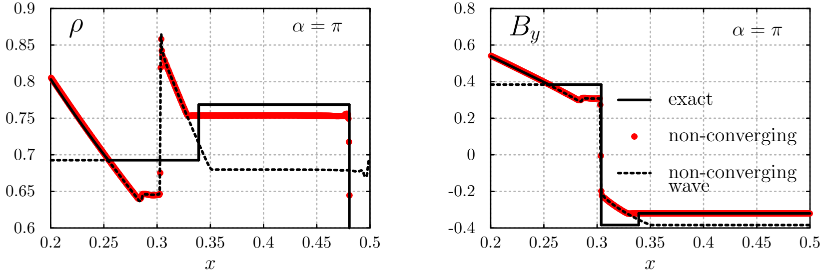

- An intermediate shock is a non-regular, i.e., not a Lax shock, wave that changes the orientation of the magnetic field.
- Slow compound wave: super-Alfvénic $\rightarrow$ sub-slow.
- In shock frame upstream: $c_a < v_n < c_f$

$$v_n = 1.0174, c_a = 0.9661, c_f = 1.1295$$

- In shock frame downstream: $v_n < c_s, c_a$

$$v_n = 0.7341, c_s = 0.8033, c_a = 0.8222$$

Non-unique solutions

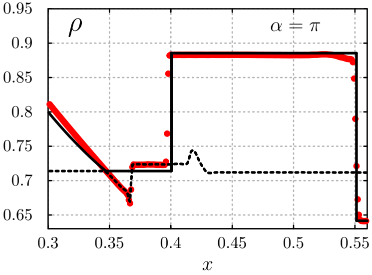

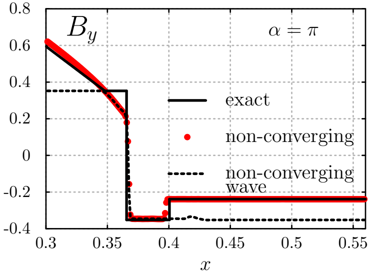

- An intermediate shock is a non-regular wave that changes the orientation of the magnetic field.
- Fast compound wave: super-fast $\rightarrow$ sub-Alfvénic.
- In shock frame upstream: $v_n > c_a, c_f$

$$v_n = 1.5868, c_a = 1.5041, c_f = 1.5401$$

- In shock frame downstream: $c_s < v_n < c_a$

$$v_n = 1.4638, c_s = 1.0766, c_a = 1.4698$$

Psuedo-convergence

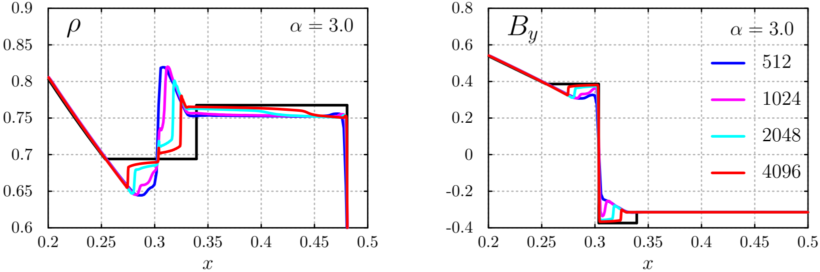

- Near-coplanar case, compound waves present at lower resolutions.
- Psuedo-convergence: increasing resolution produces convergence to regular wave solution [9].
- The compound waves begin to break apart between 1024 and 2048 grid points.
- As $\pi - \alpha$ decreases, a finer resolution is required to recover the regular wave solution.
- When $\pi = \alpha$, compound wave at all resolutions.

Psuedo-convergence

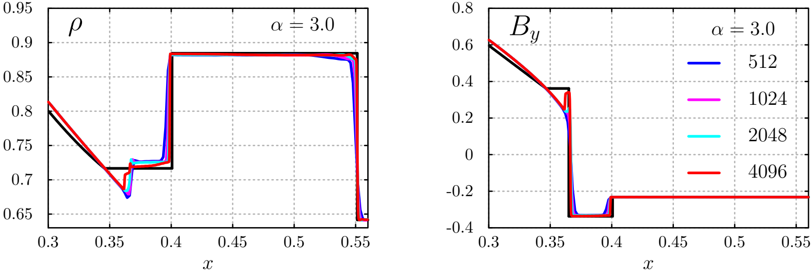

- Near-coplanar case, compound waves present at lower resolutions.
- Psuedo-convergence: increasing resolution produces convergence to regular wave solution [9].
- The compound waves begin to break apart between 1024 and 2048 grid points.
- As $\pi - \alpha$ decreases, a finer resolution is required to recover the regular wave solution.
- When $\pi = \alpha$, compound wave at all resolutions.

Compound Wave modification

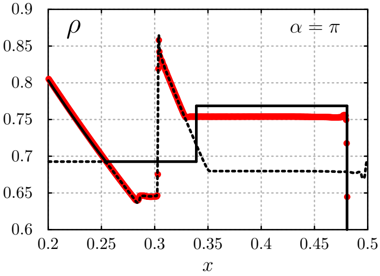

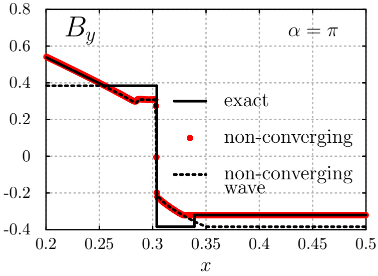

- Compound waves are product of numerical diffusion for near coplanar problems.
- Reduce diffusion to recover correct solution. How?

Compound Wave modification

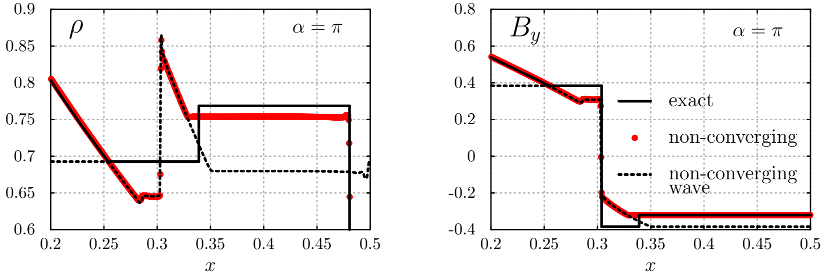

- Compound waves are product of numerical diffusion for near coplanar problems.
- Reduce diffusion to recover correct solution. How?
- ρ and B_t should remain constant across the rotational discontinuity $x = 0.303$.

Compound Wave modification

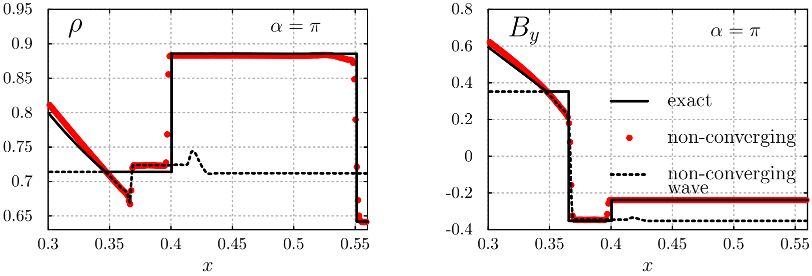

- Compound waves are product of numerical diffusion for near coplanar problems.
- Reduce diffusion to recover correct solution. How?
- ρ and B_t should remain constant across the rotational discontinuity $x = 0.375$.

Compound Wave modification

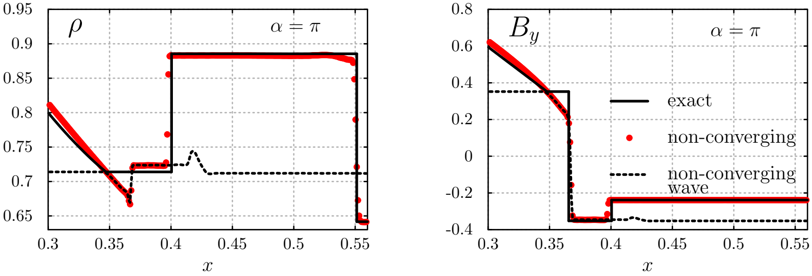

- Compound waves are product of numerical diffusion for near coplanar problems.
- Reduce diffusion to recover correct solution. How?
- ρ and B_t should remain constant across the rotational discontinuity $x = 0.375$.
- Limit flux associated with the compound wave.

Compound Wave modification

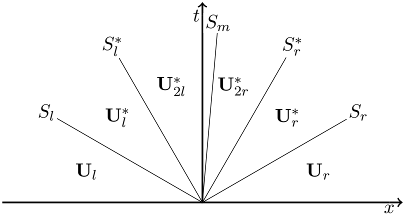

- Use HLLD to approximate intermediate states upstream and downstream of rotational discontinuity, i.e., $\mathbf{U}_\mathbf{l}^*$ and $\mathbf{U}_{2l}^*$.

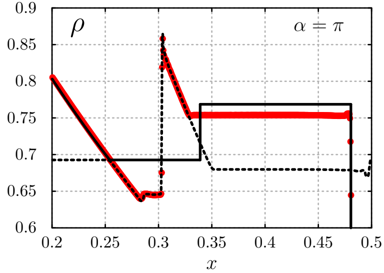

Compound Wave modification

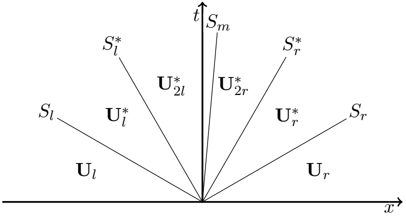

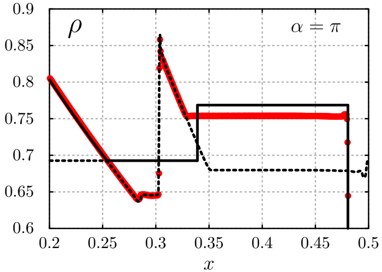

- Use HLLD to approximate intermediate states upstream and downstream of rotational discontinuity, i.e., $\mathbf{U}_l^*$ and $\mathbf{U}_{2l}^*$.
- Calculate flux $\mathbf{F}^c$ between $\mathbf{U}_l^*$ and $\mathbf{U}_{2l}^*$. This is the flux responsible for the formation of the compound wave.

Compound Wave modification

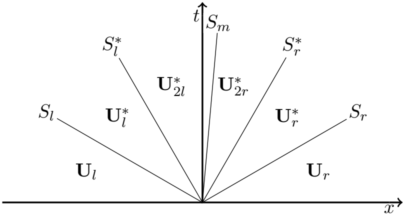

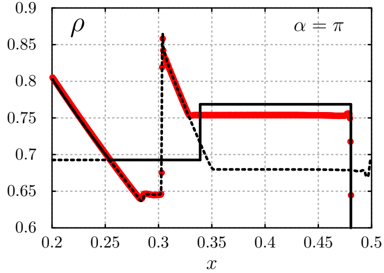

- Use HLLD to approximate intermediate states upstream and downstream of rotational discontinuity, i.e., $\mathbf{U}_\mathbf{l}^*$ and $\mathbf{U}_{2l}^*$.
- Calculate flux $\mathbf{F}^c$ between $\mathbf{U}_\mathbf{l}^*$ and $\mathbf{U}_{2l}^*$. This is the flux responsible for the formation of the compound wave.
- Reduce the contribution of $\mathbf{F}^c = \mathbf{F}(\mathbf{U}_l^*, \mathbf{U}_{l2}^*)$ to the total flux.

Compound Wave modification

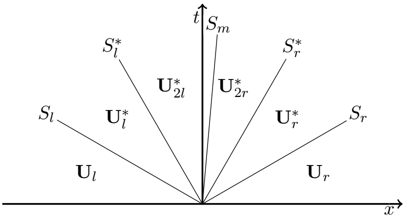

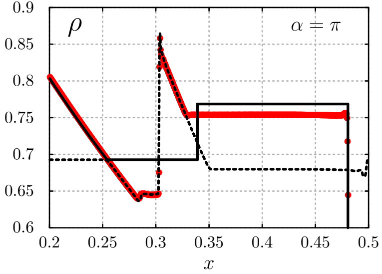

- Use HLLD to approximate intermediate states upstream and downstream of rotational discontinuity, i.e., $\mathbf{U}_\mathbf{l}^*$ and $\mathbf{U}_{2l}^*$.
- Calculate flux $\mathbf{F}^c$ between $\mathbf{U}_\mathbf{l}^*$ and $\mathbf{U}_{2l}^*$. This is the flux responsible for the formation of the compound wave.
- Reduce the contribution of $\mathbf{F}^c = \mathbf{F}(\mathbf{U}_l^*, \mathbf{U}_{l2}^*)$ to the total flux.
- $\mathbf{F} = \mathbf{F}(\mathbf{U}_l, \mathbf{U}_r) - A\mathbf{F}^c$, where $A < 0.5$.

Compound Wave modification

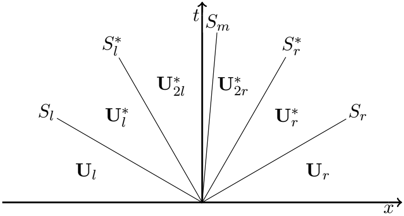

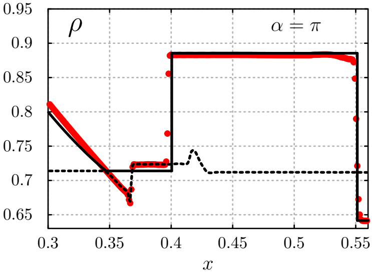

- Use HLLD to approximate intermediate states upstream and downstream of rotational discontinuity, i.e., $\mathbf{U}_\mathbf{l}^*$ and $\mathbf{U}_{2l}^*$.
- Calculate flux $\mathbf{F}^c$ between $\mathbf{U}_\mathbf{l}^*$ and $\mathbf{U}_{2l}^*$. This is the flux responsible for the formation of the compound wave.
- Reduce the contribution of $\mathbf{F}^c = \mathbf{F}(\mathbf{U}_l^*, \mathbf{U}_{l2}^*)$ to the total flux.
- $\mathbf{F} = \mathbf{F}(\mathbf{U}_l, \mathbf{U}_r) - A\mathbf{F}^c$, where $A < 0.5$.

CWM Results

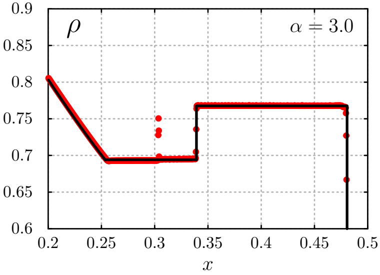

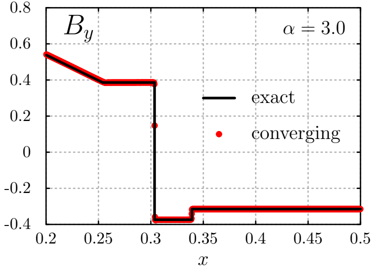

- CWM recovers the correct solution upstream and downstream of rotational discontinuity.
- Transition across rotational discontinuity is unresolved.
- Resolve it?

CWM Results

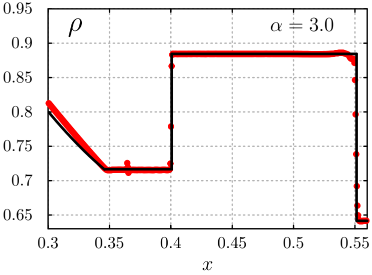

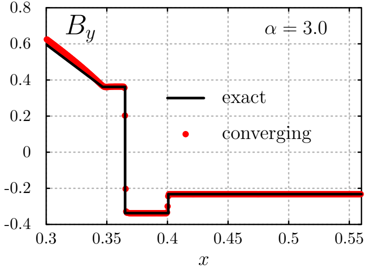

- CWM recovers the correct solution upstream and downstream of rotational discontinuity.
- Transition across rotational discontinuity is unresolved.
- Resolve it?

CWM Results

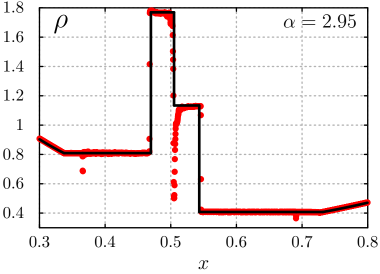

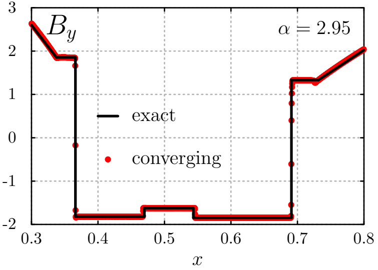

- CWM recovers the correct solution upstream and downstream of rotational discontinuity.
- Transition across rotational discontinuity is unresolved.
- Resolve it?
- Simple but non-conservative.

CWM Resolving the transition

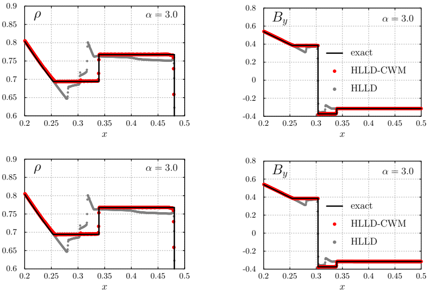

- Jump conditions in Lagrangian mass coordinates, $V = 1/\rho$, W is wave speed.
- Brackets denote difference across discontinuity.

$$
\begin{aligned}
W[V] &= -[v_n], \\
W[v_n] &= -[P - B_n^2], \\
W[\mathbf{v}_t] &= -B_n[\mathbf{B}_t], \\
W[V\mathbf{B}_t] &= -B_n[\mathbf{v}_t],
\end{aligned}
$$

CWM Resolving the transition

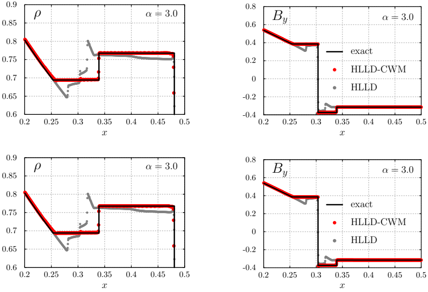

- Jump conditions in Lagrangian mass coordinates, $V = 1/\rho$, W is wave speed.
- Brackets denote difference across discontinuity.
- Across linear rotational discontinuity

$$
\begin{aligned}
[V] &= 0, \\
[v_n] &= 0, \\
[p_g] &= 0, \\
[B_t] &= 0, \\
W[\mathbf{v}_t] &= -B_n[\mathbf{B}_t],
\end{aligned}
$$

CWM Resolving the transition

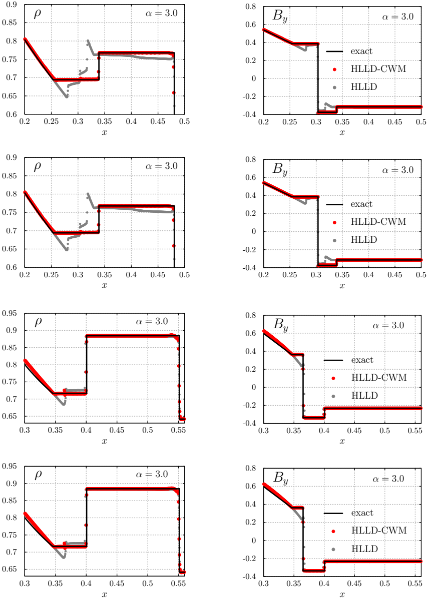

- In the case of weaker intermediate shocks, there is very little deviation at the rotational discontinuity.
- This is a desirable property of CWM. Modification applied is proportional to the strength of the shock.

CWM Resolving the transition

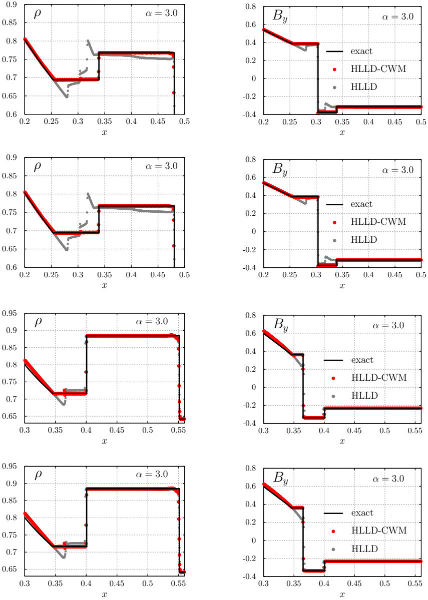

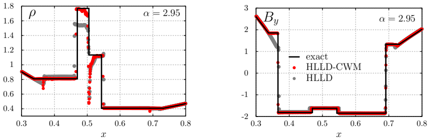

- In the case of weaker intermediate shocks, there is very little deviation at the rotational discontinuity.
- This is a desirable property of CWM. Modification applied is proportional to the strength of the shock.
- Improves result is present of other numerical errors.

Error analysis

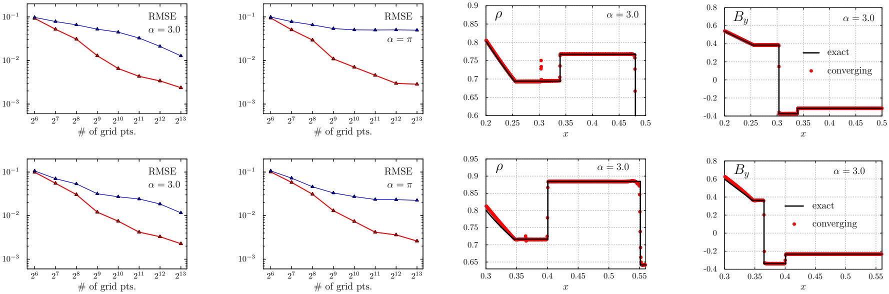

- Error calculation without applying the correction at the rotational discontinuity.
- Without CWM, the compoiund wave starts to break apart between 2^{10} and 2^{11}.
- CWM produces convergence at low grid resolutions.

Higher dimensions

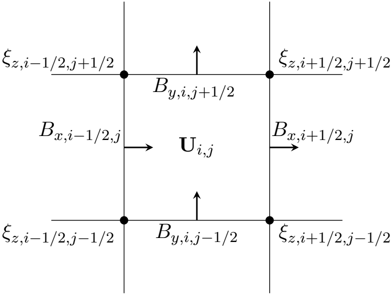

Maintaining $\nabla \cdot \mathbf{B} = 0$ with constrained transport [2].

- Staggered grid.
- Hydrodynamical variables at cell centers.
- Magnetic field at interface.
- $\mathbf{E} = -\mathbf{v} \times \mathbf{B}$ at corners.
- Denote z-component of the emf as ξ_z.

Finite area integration of interface **B**

$$B^{n+1}_{x,i+1/2,j} = B^{n}_{x,i+1/2,j} - \frac{\delta t}{\delta y}\left(\xi_{z,i+1/2,j+1/2} - \xi_{z,i+1/2,j-1/2}\right)$$

$$B^{n+1}_{y,i,j+1/2} = B^{n}_{y,i,j+1/2} + \frac{\delta t}{\delta x}\left(\xi_{z,i+1/2,j+1/2} - \xi_{z,i-1/2,j-1/2}\right)$$

Higher dimensions

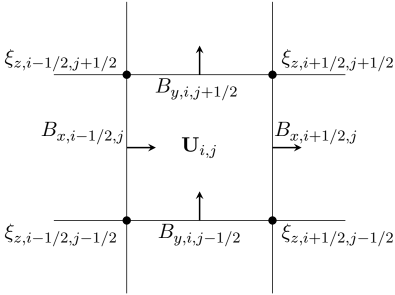

Maintaining $\nabla \cdot \mathbf{B} = 0$ with constrained transport [2].

- Staggered grid.
- Hydrodynamical variables at cell centers.
- Magnetic field at interface.
- $\mathbf{E} = -\mathbf{v} \times \mathbf{B}$ at corners.
- Denote z-component of the emf as ξ_z.

Due to perfect cancellation, the numerical divergence in the cell remains zero to machine precision.

$$(\nabla \cdot \mathbf{B})_{i,j} = \frac{1}{\delta x}\left(B_{x,i+1/2,j} - B_{x,i-1/2,j}\right) + \frac{1}{\delta y}\left(B_{y,i,j+1/2} - B_{y,i,j-1/2}\right)$$

Shared memory parallelism

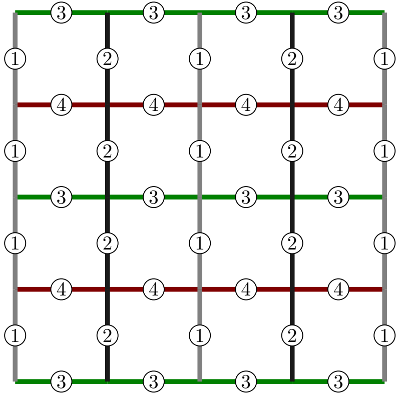

- Faces must be grouped to avoid memory contention.
- Loop over the faces becomes loop over the colors.

Shared memory parallelism

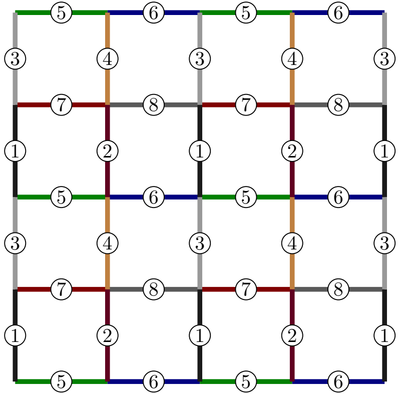

- Faces must be grouped to avoid memory contention.
- Loop over the faces becomes loop over the colors.
- With constrained transport, each face contributes to the residual at the cell center and the residual at the corner.

Efficient algorithms

```
thrust::device_vector<float> x(n);  // independent
    variable
thrust::device_vector<float> y(n);  // y = f(x)
thrust::device_vector<float> z(n);  // z = g(y)

// compute y = f(x)
thrust::transform(x.begin(),x.end(),y.begin(),f());

// compute z = g(y)
thrust::transform(y.begin(),y.end(),z.begin(),g());
```

- Function composition [3].
- $3n$ floats, $2n$ reads, $2n$ writes, and uses n temporary floats.

Efficient algorithms

```
thrust::device_vector<float> x(n);  // independent
    variable
thrust::device_vector<float> z(n);  // z = g(y) = g(
    f(x))

// compute z = g(f(x))
thrust::transform(make_transform_iterator(x.begin(),
    f()),
                  make_transform_iterator(x.end(),f
                      ()),
                  z.begin(),
                  g());
```

- Function composition [3].
- $2n$ floats, n reads, n writes, and no temporary storage.

Efficient algorithms

```
thrust::device_vector<float> x(n);  // independent
    variable
thrust::device_vector<float> z(n);  // z = g(y) = g(
    f(x))

// compute z = g(f(x))
thrust::transform(make_transform_iterator(x.begin(),
    f()),
                  make_transform_iterator(x.end(),f
                      ()),
                  z.begin(),
                  g());
```

- Function composition [3].
- $2n$ floats, n reads, n writes, and no temporary storage.

Memory access

```
struc
    conservative_variables{
  float density;
  float momentum_x;
  float energy;
}

conservative_variables
  *state;  // AoS

state[i].density =
    some_number;
state[i].momentum_x =
    another_number;
state[i].energy =
    one_more_number;
```

```
struc
    conservative_variables{
  float *density;
  float *momentum_x;
  float *energy;
}

conservative_variables
    state; // SoA

state.density[i] =
    some_number;
state.momentum_x[i] =
    another_number;
state.energy[i] =
    one_more_number;
```

- Memory coalescing occurs when multiple memory addresses are accessed with a single transaction.
- Memory does not coalesce with AoS (left).
- Memory does coalesce with SoA (right).

Memory access

```
thrust::device_vector<primitive_variables>
     primitive_state(n);  // AoS
thrust::device_vector<conservative_variables>
     conservative_state(n);    // AoS
thrust::transform_n(primitive_state.begin(),
                    primitive_state.size(),
                    conservative_state.begin(),
                    convert_primitive_to_conservative(
                        gamma));
```

- Converting from primitive variables (ρ, v_x, p_g) to conservative variables $(\rho, \rho v_x, en)$.
- No coalescing.

Memory access

```
thrust::device_vector<float> d(n),vx(n),pg(n);
thrust::device_vector<float> mx(n),en(n);
thrust::transform_n(
          thrust::make_zip_operator(
            make_tuple(d.begin(),
                       vx.begin(),
                       pg.begin())),
           n,
           thrust::make_zip_operator(
             make_tuple(d.begin(),
                        mx.begin(),
                        en.begin())),
           convert_primitive_to_conservative(gamma));
```

- Converting from primitive variables (ρ, v_x, p_g) to conservative variables $(\rho, \rho v_x, en)$.
- Arrays can be combined on the fly with a `zip_operator` to achieve coalescing.

Performance Comparison

Table: Performance comparison for Orszag-Tang [6] test.

grid size	cells/second (GPU)	cells/second (CPU)	ratio
64×64	4.1894×10^6	7.3955×10^5	5
128×128	1.6540×10^7	7.5060×10^5	22
256×256	4.4497×10^7	7.3155×10^5	60
512×512	6.3286×10^7	7.9437×10^5	79
1024×1024	7.2134×10^7	8.3354×10^5	86

- Dell Precision 7500 workstation with a (Dual CPU)
- CPU Intel Xeon E5645 @ 2.40 Ghz.
- GPU GeFroce GTX TITAN with a memory bandwidth of 288.4 GB/sec and 2688 CUDA cores.
- Almost a factor of three increase of speed ratio form 128×128 to 256×256.

Conclusion

- Provided new benchmarks for MHD model development.
- Released* a nonlinear solver for ideal MHD.
- Developed the compound wave modification:
  - First method able to produce the rotational discontinuity for coplanar Riemann problems of ideal MHD without using a nonlinear solver.
  - First method to avoid pseudo-convergence for near coplanar problems of ideal MHD.
  - FAST! HLLD intermediate states are already calculated, modification for little cost.
  - Produces the correct result when other numerical inaccuracies are present.
- Released* a high-order multi-dimensional fluid solver.
  - Algorithms implemented for general geometry on unstructured grids.
  - Capable of shared memory parallelism on GPU and CPU.
  - Can be used as blueprint or benchmark by anyone in computational physics and space weather communities wishing to increase performance.

Bibliography I

[1] B. Einfeldt. "On Godunov-Type Methods for Gas Dynamics". In: *SIAM J. Numer. Anal.* 25 (1988), pp. 294–318.

[2] C. R. Evans and J. F. Hawley. "Simulation of magnetohydrodynamic flows - A constrained transport method". In: *ApJ* 332 (Sept. 1988), pp. 659–677.

[3] Jared Hoberock and Nathan Bell. *Thrust: A Parallel Template Library*. Version 1.7.0. 2010. URL: `http://thrust.github.io/`.

[4] L. D. Landau, E. M. Lifshitz, and L. P. Pitaevskii. *Electrodynamics of continuous media*. 3rd. 1984.

[5] T. Miyoshi and K. Kusano. "A multi-state HLL approximate Riemann solver for ideal MHD". In: *J. Comp. Phys.* 208 (May 2005), pp. 315–344.

Bibliography II

[6] S. A. Orszag and C.-M. Tang. “Small-scale structure of two-dimensional magnetohydrodynamic turbulence”. In: *Journal of Fluid Mechanics* 90 (Jan. 1979), pp. 129–143.

[7] G. A. Sod. “A survey of several finite difference methods for systems of nonlinear hyperbolic conservation laws”. In: *J. Comp. Phys.* 27 (Apr. 1978), pp. 1–31.

[8] E. F. Toro, M. Spruce, and W. Speares. “Restoration of the contact surface in the HLL-Riemann solver”. In: *Shock Waves* 4 (Mar. 1994), pp. 25–34.

[9] M. Torrilhon. “Non-uniform convergence of finite volume schemes for Riemann problems of ideal magnetohydrodynamics”. In: *J. Comp. Phys.* 192 (Nov. 2003), pp. 73–94.